Neuro-Oncology Advance Access published November 15, 2012
Neuro-Oncology
doi:10.1093/neuonc/nos269
NEURO-ONCOLOGY

MicroRNA profiling in pediatric pilocytic astrocytoma reveals biologically relevant targets, including PBX3, NFIB, and METAP2

Cheng-Ying Ho, Eli Bar, Caterina Giannini, Luigi Marchionni, Matthias A. Karajannis, David Zagzag, David H. Gutmann, Charles G. Eberhart, and Fausto J. Rodriguez

Division of Neuropathology, Department of Pathology, Johns Hopkins University, Baltimore, Maryland (C.-Y.H., E.B., C.G.E., F.J.R.); Department of Laboratory Medicine and Pathology, Mayo Clinic, Rochester, Minnesota (C.G.); Cancer Biology Program, the Sidney Kimmel Comprehensive Cancer Center, Johns Hopkins University, Baltimore, Maryland (L.M.); Division of Pediatric Hematology/Oncology, Department of Pediatrics (M.A.K.); Division of Neuropathology, Department of Pathology, NYU Langone Medical Center, New York, New York (D.Z.); Department of Neurology, Washington University School of Medicine, St. Louis, Missouri (D.H.G.)

Pilocytic astrocytoma (PA) is a World Health Organization grade I glioma that occurs most commonly in children and young adults. Specific genetic alterations have been described in PA, but the pathogenesis remains poorly understood. We studied microRNA (miRNA) alterations in a large cohort of patients with PA. A total of 43 PA, including 35 sporadic grade I PA, 4 neurofibromatosis-1 (NF1)–associated PA, and 4 PA with pilomyxoid features, as well as 5 nonneoplastic brain controls were examined. *BRAF* fusion status was assessed in most cases. RNA was examined using the Agilent Human miRNA Microarray V3 platform. Expression of miRNA subsets was validated using quantitative real-time PCR (qRT-PCR) with Taqman probes. Validation of predicted protein targets was performed on tissue microarrays with the use of immunohistochemistry. We identified a subset of miRNAs that were differentially expressed in pediatric PAs versus normal brain tissue: 13 miRNAs were underexpressed, and 20 miRNAs were overexpressed in tumors. Differences were validated by qRT-PCR in a subset, with mean fold change in tumor versus brain of -17 (miR-124), -15 (miR-129), and 19.8 (miR-21). Searching for predicted protein targets in Targetscan, we identified a number of known and putative oncogenes that were predicted targets of miRNA sets relatively underexpressed in PA. Predicted targets with increased expression at the mRNA and/or protein level in PA included PBX3, METAP2, and NFIB. A unique miRNA profile exists in PA, compared with brain tissue. These miRNAs and their targets may play a role in the pathogenesis of PA.

Keywords: BRAF, glioma, microRNA, neurofibromatosis, pilocytic astrocytoma.

Pilocytic astrocytoma (PA) is a World Health Organization (WHO) grade I neoplasm representing the most frequent primary glioma among children and young adults. Most PAs have an excellent outcome after gross total resection, particularly when they arise in accessible anatomic locations, such as the cerebellum. However, a subset may behave in a more aggressive fashion and clinically progress despite the use of conventional treatments. Histologic features associated with a more aggressive course include the presence of monomorphous pilomyxoid features (ie, pilomyxoid variant)[1] and anaplasia in the form of brisk mitotic activity with or without necrosis.[2]

Recent studies have highlighted novel genetic alterations associated with PA. Tandem duplications of the *BRAF* kinase domain, leading to a *BRAF:KIAA1549* fusion, are present in most PAs.[3–10] A subset of tumors have other, usually mutually exclusive alterations, including *RAF1* rearrangements, a *FAM131B-BRAF* fusion mediated by a small interstitial deletion, or small *BRAF* insertions.[10–12] In addition, PA is the most frequent glioma in patients with neurofibromatosis type 1,[13] resulting from germline mutations in the *NF1* gene and homozygous inactivation in associated tumors, leading to RAS activation. All these genetic alterations lead to downstream activation of the MAPK signaling pathway.[14]

Received March 22, 2012; accepted September 12, 2012.

Corresponding Author: Fausto J. Rodriguez, MD, Department of Pathology, Division of Neuropathology, Johns Hopkins Hospital, Sheikh Zayed Tower, Rm M2101, 1800 Orleans St, Baltimore, MD 21231 (frodrig4@jhmi.edu).

In recent years, an increasing role for noncoding small RNA (ie, microRNA) has been uncovered in carcinogenesis. Mature microRNAs are small, single-stranded RNA molecules that bind to regulatory sequences of key mRNAs, promoting their degradation and/or inhibiting translation. In the process of carcinogenesis, the upregulation of particular microRNAs may affect tumor suppressors, whereas downregulation may allow overexpression of oncoproteins, resulting in deregulation of cell proliferation and survival.

Several microRNAs have been shown to be involved in brain tumorigenesis, including miR-21, miR-7, miR-181a/b, miR-221, and miR-222,[15–19] and seem to regulate oncogenic signaling pathways in diffuse gliomas, such as glioblastoma.[20,21] *PTEN* in particular is a key tumor suppressor gene frequently inactivated in diffusely infiltrating gliomas and may in fact be targeted, albeit not exclusively, by specific microRNAs, such as miR-21.[22] Because microRNAs may have >1 target, microRNA profiling may stratify biological and clinically relevant subgroups more accurately than conventional mRNA profiling.[23] Low-grade pediatric gliomas, such as PAs in particular, are attractive for microRNA study because they lack gross genomic alterations,[24] suggesting that undiscovered epigenetic and subtle genetic changes may contribute to their pathogenesis. In addition, microRNA profiling may lead to further, biology-based refinements in classifying histopathologically ambiguous low-grade gliomas that defy traditional classification schemes and may have prognostic or therapeutic significance.

Because of the low level of genetic instability observed in PAs, we hypothesized that epigenetic or posttranscriptional regulation may play an important role in their pathogenesis, as described in other low-grade neuroectodermal tumors, such as schwannomas.[25–27] Some studies have also highlighted a possible role for microRNAs in pediatric brain tumors,[28,29] including medulloblastoma and ependymoma.[30] A small number of PAs have also been tested for microRNA levels, which may be differentially expressed in this tumor type.[29] Furthermore, overexpression of specific microRNAs has been observed in papillary carcinoma of the thyroid, another tumor characterized by *BRAF* aberrations.[31] Identification of key microRNAs also provides a rationale for developing inhibitory RNA strategies for therapeutic purposes in patients with cancer.[32] In the current study, we investigated global microRNA expression in a large series of genetically characterized PAs, including various pathologic subtypes, followed by characterization of possible relevant biologic targets.

Methods

Patients and Tumor Samples

A total of 43 PAs were obtained from patients undergoing surgery at Johns Hopkins Hospital, New York University, or Mayo Clinic, including 35 sporadic WHO grade I PAs, 4 NF1-associated PAs, and 4 PAs with pilomyxoid features. All patients (except for 2) were ≤18 years of age at the time of surgery (median, 10 years). Nonneoplastic tissue controls included fetal cerebellum ($n = 1$) and pediatric cerebellum ($n = 1$) obtained by autopsy and cerebral cortex obtained during seizure surgery ($n = 2$) or biopsy for a nonspecific neurologic disorder with gliosis ($n = 1$). Nine additional autopsy-derived cerebellar tissue samples were included for quantitative real-time polymerase chain reaction (qRT-PCR) experiments.

Anatomic locations for tumor samples included optic pathways ($n = 10$) and supratentorial ($n = 11$) and infratentorial compartments ($n = 22$). Most tumors were previously evaluated for *BRAF* alterations as part of a separate study and by PCR and sequencing as reported.[7] Tumors were classified as aggressive if they progressed significantly within a year despite conventional therapies or recurred after gross total resections. Five patients met these criteria. Patient and tumor data are summarized in Table 1. All studies were approved by the Johns Hopkins, NYU, and Mayo Clinic Institutional Review Boards.

MicroRNA Profiling

Snap frozen fresh tumor tissue samples were used for the microRNA studies. Sample quality assessment and microarray analyses were performed at the Sidney Kimmel Comprehensive Cancer Center Microarray Core Facility at the Johns Hopkins University (Baltimore, MD). In brief, total RNA was isolated using miRNeasy Mini kits (Qiagen), followed by quality checks of both total RNA and small RNA with use of a 2100 Bioanalyzer and software that detects 28S and 18S ribosomal RNA ratio, total RNA Integrity Number, and small RNA and miRNA concentrations in the total RNA isolated. Only samples with adequate total and microRNA were used in the study.

Samples were hybridized to a Human miRNA Microarray V3 kit (G4470C, Agilent Technologies) platform previously proven to produce reproducible results as described elsewhere.[33] This array contains 866 human and 89 human viral microRNAs from the Sanger database, version 12.0. (http://microrna.sanger.ac.uk/sequences/). Each miRNA species is printed 20 times with replicate probes on the array. Total RNA (150 ng) was first dephosphorylated with 11.2 units of calf intestine alkaline phosphatase at 37°C for 30 min and followed by end-labeling with pCp-Cy3 (Agilent Technologies) and 15 units of T4 RNA ligase (GE Healthcare) at 16°C for 2 h. Labeled samples were purified using Micro Bio-Spin 6 columns (Bio-Rad). Labeling efficiency and nucleic acid concentration were measured using Nanodrop 1000. Samples were then mixed with 10x blocking agent and 2x Hi-RPM hybridization buffer (Agilent Technologies), and hybridizations were performed at 55°C with rotation at 20 rpm in a designated Agilent G2545A

Table 1. Patients and tumor characteristics

Case	Age (years)	Diagnosis	Location	Clinically Aggressive	Genetic alteration
1	6	Sporadic PA	L FRONTAL LOBE	Yes	No *BRAF* fusion[a]
2	15	Sporadic PA	BRAINSTEM	No	No *BRAF* fusion[a]
3	13	Sporadic PA	CEREBELLUM	No	*KIAA1549:BRAF* fusion
4	17	Sporadic PA	MEDULLA	No	No *BRAF* fusion[a]
5	16	Sporadic PA	L TEMPORAL	No	No *BRAF* fusion[a]
6	3	Sporadic PA	CEREBELLUM	No	*KIAA1549:BRAF* fusion
7	5	Sporadic PA	CEREBELLUM	Yes	No *BRAF* fusion[a]
8	9	Sporadic PA	CEREBELLUM	No	*KIAA1549:BRAF* fusion
9	16	Sporadic PA	POSTERIOR FOSSA	No	No *BRAF* fusion[a]
10	10	Sporadic PA	CEREBELLUM	NA	*KIAA1549:BRAF* fusion
11	11	Sporadic PA	CEREBELLUM	No	*KIAA1549:BRAF* fusion
12	15	Sporadic PA	CEREBELLUM	No	*KIAA1549:BRAF* fusion
13	11	Sporadic PA	CEREBELLUM	No	None
14	9	Sporadic PA	CEREBELLUM	No	*KIAA1549:BRAF* fusion
15	14	Sporadic PA	CEREBELLUM	No	*KIAA1549:BRAF* fusion
16	25	Sporadic PA	OPTIC CHIASM	No	*KIAA1549:BRAF* fusion
17	12	Sporadic PA	CEREBELLUM	No	*KIAA1549:BRAF* fusion
18	5	Sporadic PA	BRAINSTEM	No	*KIAA1549:BRAF* fusion
19	4	Sporadic PA	POSTERIOR FOSSA	No	*KIAA1549:BRAF* fusion
20	9	Sporadic PA	CEREBELLUM	No	None
21	20	Sporadic PA	THALAMUS	Yes	None
22	10	Sporadic PA	CERVICAL	No	*KIAA1549:BRAF* fusion
23	9	Sporadic PA	OPTIC TRACT	Yes	*KIAA1549:BRAF* fusion
24	16	Sporadic PA	TECTUM	No	*KIAA1549:BRAF* fusion
25	5	Sporadic PA	THALAMUS	No	*KIAA1549:BRAF* fusion
26	4	Sporadic PA	HYPOTHALMUS	Yes	None
27	7	Sporadic PA	THALAMUS	No	*KIAA1549:BRAF* fusion
28	6	Sporadic PA	CEREBELLUM	NA	None
29	7	Sporadic PA	MIDBRAIN/THALAMUS	No	None
30	17	Sporadic PA	L TEMPORAL LOBE	No	None
31	10	Sporadic PA	HYPOTHALMUS	No	*KIAA1549:BRAF* fusion
32	11	Sporadic PA	HYPOTHALMUS	NA	None
33	4	Sporadic PA	POST FPSSA	NA	None
34	12	Sporadic PA	THALMAUS	NA	None
35	1	Sporadic PA	CEREBELLUM	No	*BRAF*V600E
36	13	NF1-PA	R FRONTAL LOBE	No	NF1 (clinical)
37	2	NF1-PA	OPTIC NERVE	No	NF1 (clinical)
38	18	NF1-PA	OPTIC TRACT	No	NF1 (clinical)
39	18	NF1-PA	THALAMUS	NA	NF1 (clinical)
40	2	Pilomyxoid features	OPTIC PATHWAY	No	None
41	2	Pilomyxoid features	THALAMUS	No	None
42	4	Pilomyxoid features	HYPOTHALAMUS	NA	*KIAA1549:BRAF* fusion
43	1	Pilomyxoid features	HYPOTHALMUS	NA	*KIAA1549:BRAF* fusion
C1	18	Pediatric cortex	FRONTAL LOBE		ND
C2	26	Cortex	L TEMPORAL LOBE		ND
C3	4	Pediatric cortex	TEMPORAL LOBE		ND
C4	NA	Fetal brain	CEREBELLUM		ND
C5	NA	Pediatric cerebellum	CEREBELLUM		ND

Abbreviations: NA, not available; ND, not done.
[a]BRAFV600E not evaluated.

hybridization oven for 20 h. Finally, microarrays were washed and scanned using an Agilent scanner controlled by Agilent Scan Control 7.0 software. Data were acquired using Agilent Feature Extraction 9.5.3.1 software for miRNA microarray, generating a GeneView file that contains summarized signal intensities for each miRNA by combining intensities of replicate probes and background subtraction.

MicroRNA Data Analysis

Data normalization and analysis were performed using GeneSpring GX, version 11, according to the standard software recommendations (Agilent Technologies). In brief, miRNA signal intensities from GeneView files were subjected to quantile normalization. Expression differences were compared using the *t* test unpaired unequal variance (Welch) between pairs of interest. An adjusted *P*-value was obtained using the Benjamini-Hochberg false discover rate for multiple comparisons.

MicroRNA Validation

Validation of selected targets (mature miR-21, miR-124, mir-129) was performed using Taqman microRNA assays (Applied Biosystems) according to the manufacturer's recommendations. All samples were tested in triplicate using 96-well plates. The noncoding small nuclear RNA U6 was used as internal control. Wells lacking template were used as negative controls. Expression changes were compared by relative quantification in the form of fold changes obtained with the ΔΔCt method.[34]

MicroRNA Target Prediction

Predicted mRNA targets for differentially expressed microRNAs were obtained from the TargetScan Human online database (release 6.0). With the use of this strategy, microRNA targets are predicted by matching the seed region of the specific microRNA with conserved 8mer and 7mer sites as described elsewhere[35] (http://www.targetscan.org).

Analysis of Functional Annotation Results

We tested the association between the lists of mRNA targets for differentially selected miRs and relevant cancer signaling pathways available from the NCI Pathway Commons database via analysis of functional annotation, as previously described.[36] In brief, the χ^2 test was used to identify the specific signaling pathways significantly over-represented among the genes targeted by the microRNAs differentially expressed in PA. The Benjamini-Hochberg method was applied to correct the obtained *P* values for multiple testing, and a false discovery rate of $<5\%$ was considered to be statistically significant.

Gene Expression Analysis

Differences in candidate mRNA targets were studied using data files obtained with Affymetrix HG-U133 Plus 2.0 chips. Sources included newly profiled 17 sporadic PAs (5 of which were also subjected to microRNA analysis) and 1 nonneoplastic cortex; 47 PA samples from our previously reported study[37] and 19 normal brain samples from various anatomic regions (cerebral cortex [$n = 4$], occipital lobe [$n = 4$], cerebellum [$n = 3$], and hypothalamus [$n = 8$]) obtained from a publicly available dataset at the NCBI gene expression omnibus (GSE7307). Raw gene expression data preprocessing and normalization were performed at the probe level with the use of the Frozen Robust Multi-Array Analysis approach described by McCall et al.[38]

Tissue Microarray (TMA) and Immunohistochemistry

Validation of protein targets was performed using 3 PAs and 1 diffuse glioma TMA containing 103 sporadic PAs, 17 NF1-associated PAs, 15 anaplastic PAs, and 79 diffuse gliomas of various grades. TMAs contained 3–4 cores per tumor. Immunohistochemical studies were performed using the following antibodies: PBX3 (Clone 1A11, LifeSpan BioSciences; 1:400), METAP2 (Rabbit polyclonal, Abnova; 1:50), and NFIB (Clone 2D6, LifeSpan BioSciences; 1:100). Immunohistochemical stains were scored by 2 independent observers (F.J.R. and C.H.) with use of the following semiquantitative scale that combined staining intensity and number of positive cells: 3 + (strong immunoreactivity in $>50\%$ tumor cells), 2 + (medium to weak immunoreactivity in 50%–100% of cells or strong immunoreactivity in 10%–50% tumor cells), 1 + (strong immunoreactivity in 1%–10% or medium to weak immunoreactivity in 10%–50% tumor cells), and 0 = negative. For PBX3 and NFIB, only nuclear reactivity was considered to be significant, whereas only cytoplasmic METAP2 reactivity was scored. The χ^2 or Fisher's exact test was used to compare proportions, and Student's *t* test or Wilcoxon rank sum was used to compare quantitative variables. All tests were 2-sided with *P* values $<.05$ considered to be statistically significant.

Results

A Subset of microRNAs Is Differentially Expressed in Pediatric PAs

Comparisons were made between tumors and nonneoplastic brain, as well as different tumor subsets. The most robust differences were evident between tumors as a group and nonneoplastic brain tissues, as shown by unsupervised hierarchichal clustering (Fig. 1). The volcano plot comparing tumor tissue and nonneoplastic brain using an adjusted *P*-value of.05 and fold change of 2 as cutoffs revealed 13 human microRNAs relatively underexpressed in tumors (Table 2) and 18 overexpressed (Table 3) (Fig. 2). Next, we tested a subset of

Fig. 1. A subset of microRNAs is differentially expressed between pilocytic astrocytomas (PAs) and nonneoplastic brain. Heatmap illustrates expression differences between PAs and nonneoplastic brain, as shown by hierarchical clustering. The nonneoplastic brain controls, representing cortex (C1-3), and fetal (C4) and pediatric cerebellum (C5) (box). Data were obtained using the Agilent miRNA Microarray V3 kit platform.

Table 2. MicroRNAs relatively underexpressed in tumor tissue compared with non-neoplastic brain

SystematicName	Corrected *P* value	*P* value	Fold Change
hsa-miR-124	.02	4.39E-04	67.40
hsa-miR-129*	.04	.001513	22.60
hsa-miR-129-3p	6.50E-04	4.70E-06	54.25
hsa-miR-129-5p	.006	6.74E-05	35.07
hsa-miR-138-2*	.01	2.01E-04	2.83
hsa-miR-181a	.04	.001238	2.95
hsa-miR-323-3p	.03	9.26E-04	2.53
hsa-miR-329	.04	.001171	2.48
hsa-miR-383	.02	3.58E-04	14.71
hsa-miR-490-3p	.006	7.30E-05	10.76
hsa-miR-490-5p	.05	.002093	2.75
hsa-miR-7	.02	6.42E-04	20.54
hsa-miR-873	.02	4.77E-04	26.30

Table 3. MicroRNAs relatively overexpressed in tumor tissue, compared with nonneoplastic brain

SystematicName	Corrected *P* value	*P* value	Fold change
hsa-let-7c*	6.50E-04	4.74E-06	2.69
hsa-miR-10b	2.60E-10	2.71E-13	17.79
hsa-miR-10b*	.02	4.75E-04	3.58
hsa-miR-1260	.004	3.77E-05	2.50
hsa-miR-1274a	.02	5.10E-04	2.17
hsa-miR-1288	.01	2.29E-04	3.28
hsa-miR-142-3p	.02	4.24E-04	4.65
hsa-miR-143*	4.65E-04	1.45E-06	2.02
hsa-miR-146b-5p	.04	.001	2.42
hsa-miR-155	6.50E-04	4.72E-06	4.08
hsa-miR-21	.04	.002	18.55
hsa-miR-21*	.01	2.25E-04	30.37
hsa-miR-23a	.02	5.76E-04	3.21
hsa-miR-542-5p	.04	.001	4.62
hsa-miR-650	.03	8.54E-04	3.71
hsa-miR-886-3p	.004	4.64E-05	5.53
hsa-miR-92b	.04	.001	2.07
hsa-miR-92b*	3.73E-08	7.77E-11	2.25

the cases (9 sporadic PA, 5 nonneoplastic brains) for hsa-miR-124, hsa-miR-129, and hsa-miR-21 with use of quantitative PCR. Mean miR-124 expression fold change in tumor versus brain was -17 ($P = .006$), for miR-129 was -15 ($P = .009$), and for miR-21 was 19.8 ($P = .003$) (Fig. 3A–C). Next, we expanded the control group to include 9 additional nonneoplastic cerebellar examples and also tested the 4 NF1-PAs. The lowest expression of miR-124 and miR-129 was actually present in the NF1-PA group, compared with sporadic PA and nonneoplastic brain, whereas the converse was true for miR-21 (Fig. 3D–F). These last differences were also present in the initial Agilent array profiling experiments (not shown).

Differentially Expressed MicroRNA in NF1-Associated Versus BRAF Fusion–Positive Tumors

We also searched for specific differences in hsa-microRNA expression among different PA groups, in particular, by anatomic location, pathologic subtype, genetic background, and clinical aggressiveness, although the differences were not as robust as between tumor and nonneoplastic brain. A volcano plot using an adjusted *P* value of .05 and fold change of 2 demonstrated 4 microRNAs differentially expressed between NF1-associated and tumors with *BRAF* alterations: hsa-miR-650 and hsa-miR-1276 were differentially overexpressed in NF1 tumors (3.7-fold), whereas hsa-miR-744* and hsa-miR-187* were underexpressed (2- and 2.5-fold). However, the overall expression levels of these microRNAs were relatively low, and further validation of miR-650 by qRT-PCR was noncontributory (data not shown). These findings suggest that expression differences between NF1-PA and sporadic PA may exist at the miRNA level in addition to the mRNA level as previously reported.[37]

Biologically Relevant MicroRNA Targets in PAs

We used the online program TargetScan to discover target mRNAs for microRNAs differentially expressed in PAs. A total of 36 mRNAs were predicted targets of ≥4 microRNAs differentially underexpressed in PAs, compared with brain, several encoding known, and putative oncoproteins (Table 4), whereas 10 mRNAs were predicted targets for microRNAs differentially overexpressed in PAs (Table 5). We searched for these predicted mRNAs in a combined dataset containing a total of 64 PA and 20 normal brain samples representing different anatomical regions. Most of these predicted targets were overexpressed in PA, compared with normal brain, and unsupervised clustering demonstrated clear separation between tumor and brain samples (Fig. 4). Conversely, none of the mRNAs-predicted targets of overexpressed microRNAs in PA were underexpressed. When searching for genes differentially expressed in *NF1* versus *BRAF* altered tumors, Targetscan search revealed 7 genes that were predicted targets of the overexpressed microRNAs (miR-650 and miR-1276) (Table 6). There were no combined predicted targets of hsa-miR-744 and hsa-miR-187.

Next, we performed analysis of functional annotation to compare microRNA PA targets with signaling pathways. Of interest, many of the gene sets identified for 2 of the microRNAs with the lowest differential expression (miR-124 and miR-129–5p) targeted multiple components of receptor tyrosine kinase/MAPK/ERK signaling pathways (Supplementary Tables 1 and 2).

Because microRNAs may have a more important role in interfering with protein translation, we further tested candidate targets by immunohistochemistry with use of commercially available antibodies. From the cases studied for microRNA expression by qRT-PCR, paraffin sections were available for 5 tumors and 3 cerebral cortex controls. Most of these cases underexpressed

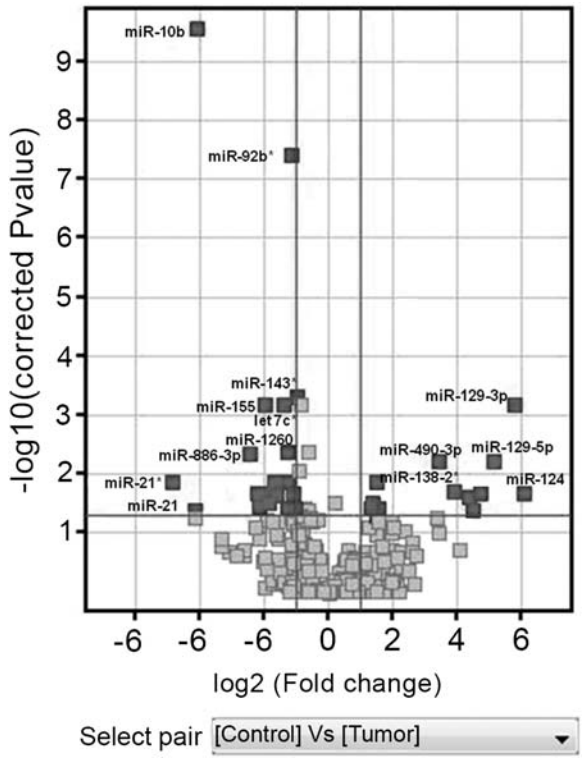

Fig. 2. Differential microRNA expression in PAs, compared with nonneoplastic brain. Volcano plot shows microRNA expression differences between PA and nonneoplastic brain based on a cutoff value of 2-fold differential expression and adjusted $P < .05$.

miR-124 (-3.5- to -67-fold) and miR-129 (-1.33- to -772.16-fold), compared with normal brain. In this subset, 5 (of 5) tumor samples showed increased (moderate to marked expression) of the corresponding predicted targets PBX3 and NFIB, whereas 2 (of 5) tumors showed increased expression of METAP2. In this limited dataset, the tightest inverse correlation was noted between miR-124 expression and NFIB IHC ($R^2 = 0.47$, $P = .05$), followed by miR-129 and NFIB ($R^2 = 0.30$) and miR-129 and PBX3 ($R^2 = 0.23$). A linear correlation between miR-124 and METAP2 was not observed ($R^2 = 0.006$).

Next, we searched for expression differences of these proteins in a large set of independent tumors obtained from 4 different microarrays. We identified strong (3+)PBX3 nuclear staining in most PAs, independent of subtype when compared with nonneoplastic brain and diffuse gliomas ($P < .001$) (Fig. 5) (Table 7). Cytoplasmic METAP2 was expressed most strongly in NF1-associated PAs, compared with sporadic PAs ($P < .001$), and less so in sporadic examples, which in turn were mildly overexpressed, compared with diffuse gliomas and nonneoplastic brain ($P = .001$) (Fig. 5) (Table 7). Strong (3+) nuclear NFIB labeling was also highest in anaplastic PAs, followed by sporadic PAs, compared with nonneoplastic brain and diffuse gliomas ($P < .001$). The κ statistics comparing the scores from each observer were 0.25 (PBX3), 0.26 (NFIB), and 0.37 (METAP2), reflecting fair agreement on each. Of importance, the major differences between

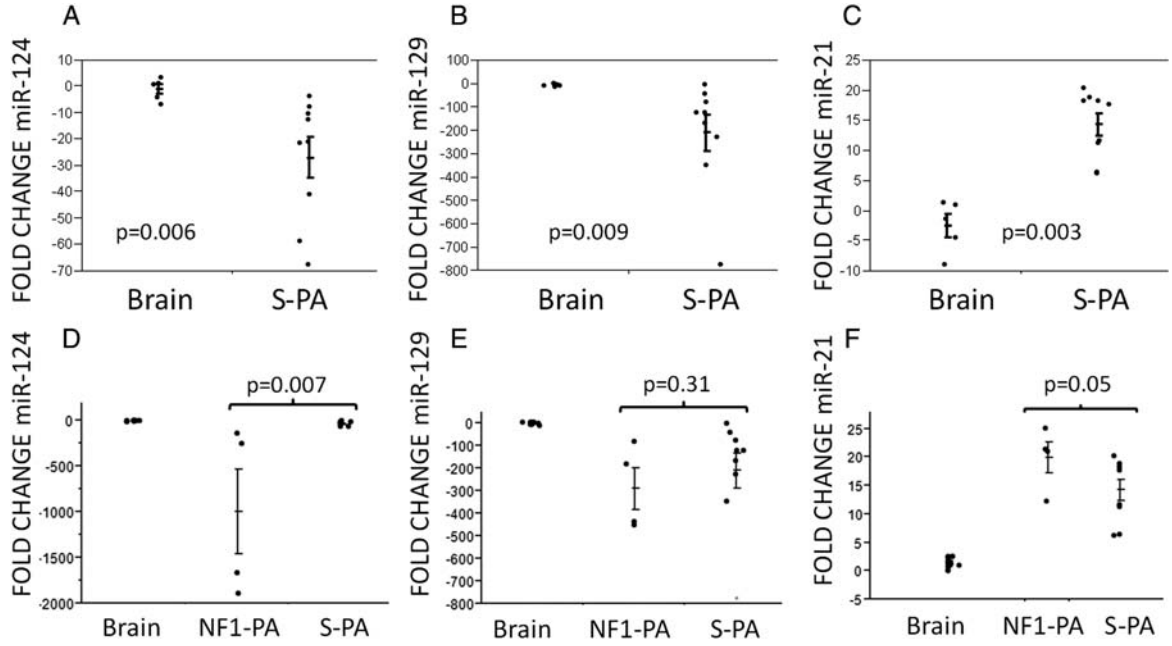

Fig. 3. Differential expression of microRNAs between PAs and nonneoplastic brain confirmed by qRT-PCR. miR-124 (A) and miR-129 (B) were relatively underexpressed in sporadic PA ($n = 9$), compared with nonneoplastic brain (pediatric cerebellum [$n = 1$], cortex [$n = 3$], and fetal cerebellum [$n = 1$]), and miR-21 was relatively overexpressed (C) in an internal validation experiment. In addition, independent nonneoplastic cerebellar samples and the 4 NF1-associated PAs were analyzed. The lowest expression of miR-124 (D) and miR-129 (E) was evident in NF1-PA ($n = 4$), compared with sporadic PA ($n = 9$) and nonneoplastic brain controls (cortex [$n = 3$], cerebellum [$n = 11$]). An opposite effect was observed with miR-21 (F). Each dot represents the mean of 3 replicates. Error bars are shown. *P*-values were obtained using the Wilcoxon rank sum test.

Table 4. Predicted Targetscan protein targets by microRNAs underexpressed in pilocytic astrocytoma (PA)

Target Gene	Gene Name	Representative microRNA					
BACH2	BTB and CNC homology 1, basic leucine zipper transcription factor 2	miR-124	miR-129-5p	miR-323-3p	miR-490-3p		
BCL7A	B-cell CLL/lymphoma 7A	miR-124	miR-129-3p	miR-329	miR-873		
BMPR2	bone morphogenetic protein receptor, type II (serine/threonine kinase)	miR-129-3p	miR-129-5p	miR-181a	miR-329	miR-490-5p	miR-873
BRWD1	bromodomain and WD repeat domain containing 1	miR-124	miR-129-3p	miR-129-5p	miR-7		
DDX3X	DEAD (Asp-Glu-Ala-Asp) box polypeptide 3, X-linked	hsa-miR-124	miR-129-5p	miR-181a	miR-323-3p		
FAM135B	family with sequence similarity 135, member B	-miR-124	miR-129-3p	miR-129-5p	miR-490-3p		
FOXN3	forkhead box N3	miR-129-5p	miR-323-3p	miR-329	miR-383	miR-7	
G3BP2	GTPase activating protein (SH3 domain) binding protein 2	miR-124	miR-181a	miR-323-3p	miR-7		
GLIS3	GLIS family zinc finger 3	miR-129-5p	miR-181a	miR-323-3p	miR-383		
HIC2	hypermethylated in cancer 2	miR-129-5p	miR-181a	miR-490-3p	miR-873		
HIPK2	homeodomain interacting protein kinase 2	miR-124	miR-129-3p	miR-181a	miR-490-5p	miR-7	
HNRNPA1	heterogeneous nuclear ribonucleoprotein A1	miR-129-5p	miR-323-3p	miR-383	miR-490-3p		
KIAA0182	KIAA0182	miR-129-3p	miR-129-5p	miR-181a	miR-7		
KIAA2018	KIAA2018	miR-124	miR-129-5p	miR-181a	miR-7		
KLF12	Kruppel-like factor 12	miR-129-3p	miR-323-3p	miR-329	miR-7		
KLHL28	kelch-like 28 (Drosophila)	miR-124	miR-129-3p	miR-129-5p	miR-7		
KPNA6	karyopherin alpha 6 (importin alpha 7)	miR-129-5p	miR-490-5p	miR-7	miR-873		
MECP2	methyl CpG binding protein 2 (Rett syndrome)	miR-129-5p	miR-181a	miR-7	miR-873		
METAP2	methionyl aminopeptidase 2	miR-124	miR-181a	miR-323-3p	miR-490-5p		
MOBKL1A	MOB1, Mps One Binder kinase activator-like 1A (yeast)	miR-124	miR-323-3p	miR-490-3p	miR-7		
NFIB	nuclear factor I/B	miR-124	miR-129-5p	miR-323-3p	miR-490-5p	miR-7	miR-873
NR2C2	nuclear receptor subfamily 2, group C, member 2	miR-129-5p	miR-181a	miR-329	miR-490-3p		
PBX3	pre-B-cell leukemia homeobox 3	miR-129-5p	miR-181a	miR-323-3p	miR-7		
PHF21A	PHD finger protein 21A	miR-129-3p	miR-129-5p	miR-383	miR-7		
PRPF40A	PRP40 pre-mRNA processing factor 40 homolog A (S. cerevisiae)	miR-124	miR-129-5p	miR-323-3p	miR-490-5p		
PTAR1	protein prenyltransferase alpha subunit repeat containing 1	miR-124	miR-129-3p	miR-129-5p	miR-329	miR-7	
SFRS18	splicing factor, arginine/serine-rich 18	miR-129-3p	miR-181a	miR-323-3p	miR-490-5p		
SP1	Sp1 transcription factor	miR-124	miR-181a	miR-329	miR-7		
ST8SIA4	ST8 alpha-N-acetyl-neuraminide alpha-2,8-sialyltransferase 4	miR-124	miR-129-3p	miR-181a	miR-383		
TET3	tet oncogene family member 3	miR-124	miR-129-3p	miR-490-3p	miR-873		
TNRC6B	trinucleotide repeat containing 6B	miR-124	miR-129-3p	miR-129-5p	miR-181a	miR-323-3p	miR-7
TRPS1	trichorhinophalangeal syndrome I	miR-124	miR-129-3p	miR-129-5p	miR-323-3p	miR-383	miR-490-5p
WIPF2	WAS/WASL interacting protein family, member 2	miR-124	miR-329	miR-383	miR-7		
XYLT1	xylosyltransferase I	miR-124	miR-129-3p	miR-181a	miR-323-3p		
ZNF148	zinc finger protein 148	miR-124	miR-129-3p	miR-323-3p	miR-7		
ZNF395	zinc finger protein 395	miR-129-5p	miR-323-3p	miR-490-3p	miR-7		

Table 5. Predicted Targetscan protein targets of microRNAs overexpressed in pilocytic astrocytoma

Target Gene	Gene Name	Representative miRNA			
ABL2	v-abl Abelson murine leukemia viral oncogene homolog 2 (arg, Abelson-related gene)	miR-1274a	miR-142-3p	miR-143	miR-23a
CBL	Cas-Br-M (murine) ecotropic retroviral transforming sequence	miR-1288	miR-143	miR-155	miR-650
GATAD2B	GATA zinc finger domain containing 2B	miR-1260	miR-155	miR-21	miR-650
KCNA1	potassium voltage-gated channel, shaker-related subfamily, member 1 (episodic ataxia with myokymia)	miR-1274a	miR-155	miR-21	miR-650
MLL2	myeloid/lymphoid or mixed-lineage leukemia 2	miR-1260	miR-143	miR-146b-5p	miR-23a
NFIX	nuclear factor I/X (CCAAT-binding transcription factor)	miR-10b	miR-1260	miR-23a	miR-886-3p
NOVA1	neuro-oncological ventral antigen 1	miR-1274a	miR-143	miR-146b-5p	miR-155
PURB	purine-rich element binding protein B	let-7c	miR-142-3p	miR-21	miR-23a
SLC39A10	solute carrier family 39 (zinc transporter), member 10	miR-142-3p	miR-143	miR-155	miR-23a
TRPS1	trichorhinophalangeal syndrome I	miR-1274a	miR-143	miR-155	miR-23a

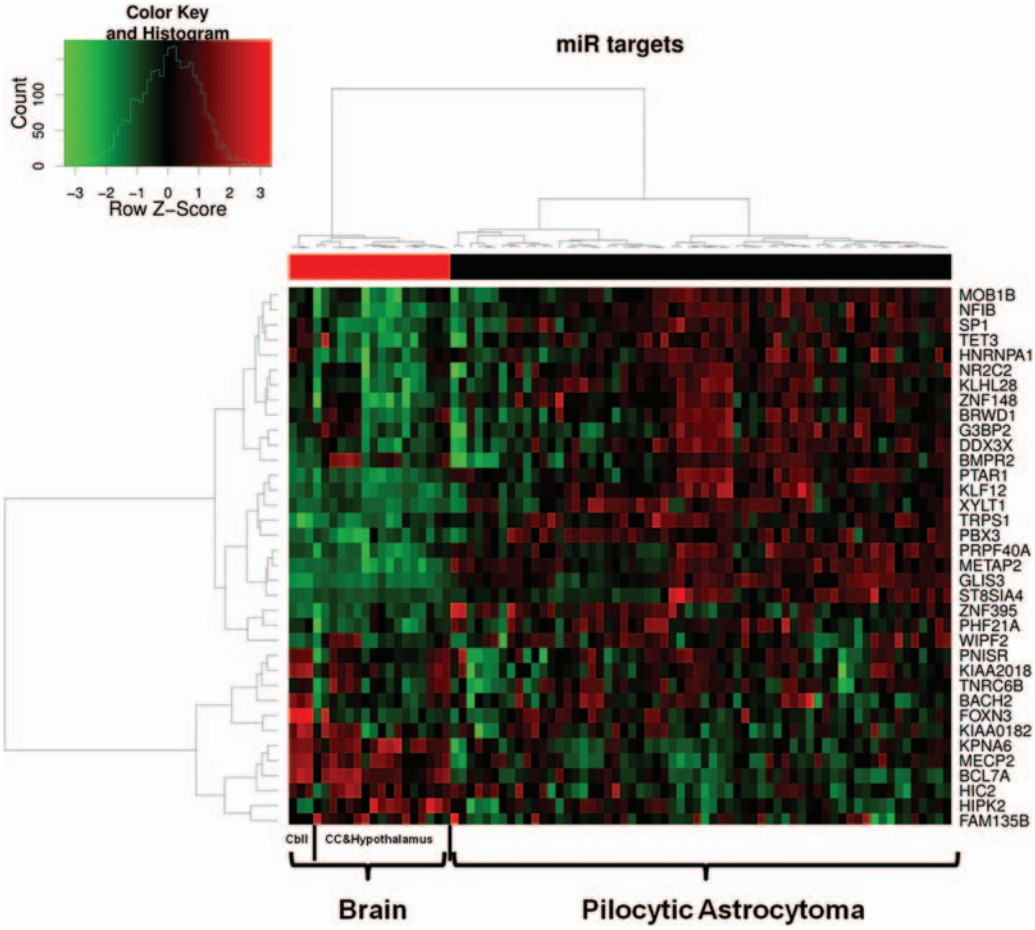

Fig. 4. microRNA predicted mRNA target differences in PAs and nonneoplastic brain samples. Unsupervised hierarchical clustering of normal brain and PA cases according to the expression of the genes targeted by the identified microRNAs down-regulated in PA (profiling by Affymetrix HG-U133 Plus 2.0 chips). Target genes are shown by row, and the different samples are shown by column. A total of 64 PAs was studied. Nonneoplastic controls included cerebral cortex (CC; $n = 9$), hypothalamus ($n = 8$), and cerebellum (CbII; $n = 3$). The centered Pearson's distance and the Ward's clustering methods were used. The color scale represents increased (red) or decreased (green) gene expression.

Table 6. Predicted Targetscan protein targets of microRNAs overexpressed in NF1-PA versus PA with BRAF alterations

Target Gene	Gene Name	Representative miRNA	
ANP32E	acidic (leucine-rich) nuclear phosphoprotein 32 family, member E	miR-1276	miR-650
CTNND1	catenin (cadherin-associated protein), delta 1	miR-1276	miR-650
KPNA6	karyopherin alpha 6 (importin alpha 7)	miR-1276	miR-650
NFASC	neurofascin homolog (chicken)	miR-1276	miR-650
NUDT10	nudix (nucleoside diphosphate linked moiety X)-type motif 10	miR-1276	miR-650
ONECUT2	one cut homeobox 2	miR-1276	miR-650
RYBP	RING1 and YY1 binding protein	miR-1276	miR-650

the groups were also reflected in the individual scores from each observer (data not shown).

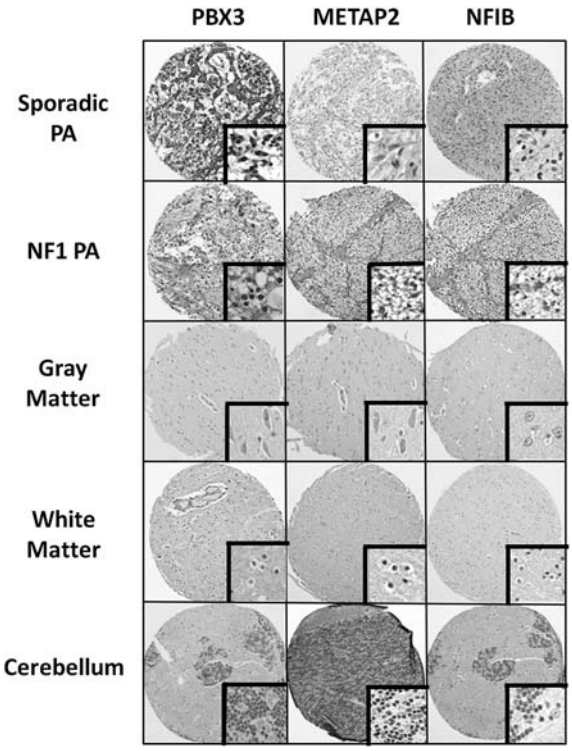

Fig. 5. microRNA protein target differences in PAs and nonneoplastic brain samples. Proteins that were predicted to be targets of differentially underexpressed microRNAs in PAs included putative oncogenes, such as PBX3, METAP2, and NFIB. With use of immunohistochemistry on tissue microarray sections, PBX3 and NFIB demonstrated strong nuclear staining in PAs, compared with brain, and METAP2 demonstrated modest cytoplasmic staining in a subset of PAs and was strongest in NF1-associated PAs.

Discussion

Numerous roles have been proposed and studied for microRNA in physiologic and pathologic states, including cancer. MicroRNA regulation has been a fruitful area of research in brain cancer, particularly glioblastoma. In fact, extensive post-transcriptional regulatory networks in this specific tumor type, in which microRNAs are key components, have emerged using bioinformatic and experimental approaches.[20]

However, less is known about microRNA regulation of low-grade gliomas and PAs in particular. MicroRNA and mRNA profiling studies using 4 PA samples have demonstrated clustering for PAs separate from other pediatric brain tumors.[28,29] In a study of WHO grade I–III astrocytomas, Li et al. identified a number of microRNAs to be underexpressed in all glioma grades, compared with brain, including miR-124,[21] which in our study, was also differentially underexpressed.

miR-21 seems to target multiple components of key tumor suppressor and anti-apoptotic pathways, including p53, transforming growth factor beta, and mitochondria,[39–42] as well as matrix metalloproteinases, which contribute to invasion in glioma.[43] Elevation of miR-21 has been found in a variety of tumor types, compared with normal tissues, and highlights the potential of microRNA to serve as glioma biomarkers (eg, in cerebrospinal fluid samples).[44] One important (but not exclusive) target of miR-21 is PTEN, a key suppressor of the PI3K/AKT/mTOR pathway. PTEN loss is a frequent molecular property of high-grade gliomas, and we have previously observed decreased levels in PAs with aggressive histologic features.[45]

One of the main patterns identified in the current study is relative underexpression of a subset of microRNAs in PAs, compared with nonneoplastic brain, several of which may target known and putative oncogenes. MiR-124 is enriched in brain tissue, is downregulated in glioblastoma, and negatively affects glioblastoma proliferation and migration in vitro.[21,46] Several miR-129 cluster members were underexpressed in PAs in our study. Other investigators have also found this microRNA to be underexpressed in pediatric brain tumors, including 4 PAs.[28]

We also found increased gene expression and protein levels of putative oncogenes that may be important in the biology of PA and appeared to be targets of microRNA sets relatively underexpressed in PAs, compared with nonneoplastic brain. This is a novel aspect of our study, because these oncoproteins have not been associated with PA previously but may provide insights into low-grade glioma biology. Many oncoproteins in pediatric brain tumors play essential roles during central nervous system development. For example, PBX3 (pre–B cell leukemia homeobox 3) is one member of a group of PBX transcription factors belonging to the TALE (3 amino acid loop extension) homeobox gene family. They seem to play important developmental roles and affect gene signatures associated with

Table 7. Differential expression of putative microRNA targets in pilocytic astrocytoma (PA) identified by immunohistochemistry

Protein target	Staining pattern	Sporadic PA	NF1-PA	Anaplastic PA	Diffuse Glioma	Non-neoplastic brain
PBX3[a]	Nuclear	57/99 (58%)	11/16 (69%)	7/12 (58%)	5/79 (6%)	0/16
METAP2[a]	Cytoplasmic	25/102 (25%)	12/15 (80%)	6/13 (46%)	6/79 (4%)	0/17
NFIB[a]	Nuclear	30/95 (35%)	4/15 (27%)	5/12 (42%)	0/79	0/15

[a]Number of tumors with strong diffuse expression (3+ scores)/total number (percentage) representing the median estimate from 2 independent observers.

cancers, particularly of hematolymphoid origin. In the nervous system, *PBX3* is expressed in many anatomical regions during development, including areas of the medulla oblongata responsible for respiration control.[47] In fact, *Pbx3* null mice die from central respiratory failure.[47] Pbx3 also seems to be important in the development of a subset of glutaminergic neurons in the developing dorsal horn of the spinal cord in murine studies[48] and the striatum and intercalated cell masses of the amygdala in monkey and rat.[49,50]

Recent studies have described post-transcriptional regulation of PBX3 in cancer, particularly by microRNAs. Downregulation of miR-181a and upregulation of a gene expression signature that includes *PBX3* was associated with an adverse outcome in cytogenetically abnormal acute myeloid leukemia.[51] However, PBX3 has been found to also play a role in nonlymphoid malignancies, including prostate cancer, in which it may be regulated by a different microRNA (eg, Let 7d) in response to androgen.[52] In the current study, we identified underexpression of miR-181a and increased *PBX3* mRNA and protein levels in PAs, compared with normal brain. Furthermore, PBX3 nuclear staining was higher in PAs, compared with diffuse gliomas, which raises the possibility that PBX3 may play a relatively specific role in PAs, compared with other gliomas. However, this finding will require further confirmation by alternative methods, functional experiments, and independent samples in the future.

In the current study, a subset of underexpressed microRNAs also had methionine aminopeptidase 2 (METAP2) as a predicted target. METAP2 functions include facilitation of protein translation,[53] probably by protecting eukaryotic initiation factor 2 from inhibition by phosphorylation.[54] When evaluating protein levels by immunohistochemistry, the highest levels were present in NF1-associated PAs, with a more modest elevation in some sporadic PAs. Of relevance to our study, METAP2 was identified to be elevated in the cerebrospinal fluid of mice with optic gliomas and NF1-associated PAs in human and murine optic glioma tissue.[54] In the same study, METAP2 was not overexpressed in *Tsc1*-deficient mouse brains or TSC-associated tumors, nor was it overexpressed in the small number of sporadic PA examined; therefore, increased levels were a consequence of neurofibromin loss and a property of NF1-associated tumors. METAP2 represents an attractive therapeutic target, because it is inactivated by fumagillin, a known fungal toxin.[55] METAP2 mRNA and/or protein overexpression has been reported in several cancers, including cholangiocarcinoma,[56] colorectal carcinoma,[57] and mesothelioma.[58] Fumagillin also inhibits hepatocellular carcinoma growth in vivo,[59] and pharmacologic inhibition of METAP2 also inhibits melanoma growth.[60]

Another predicted target of a subset of underexpressed microRNAs with increased mRNA and protein levels in PAs was NFIB. NFIB, a CCAAT box-binding transcription factor, has been implicated as an oncogene in other tumors, being amplified in small cell carcinoma of the lung,[61] is overexpressed in breast cancer subsets,[62] and is involved in a novel fusion in salivary gland tumors and adenoid cystic carcinoma of the breast.[63,64] In addition, NFIB was functionally validated as a target of miR-124, with a number of proteins being downregulated by miR-124 introduction in cultured HeLa cells at the protein and mRNA level, including NFIB.[65] Of interest, we saw an inverse correlation between miR-124 and NFIB extent of expression in the limited number of cases tested (5 S-PA and 3 brain controls).

Our results highlight the complementary value of microRNA profiling in the identification of biologically relevant targets in pediatric low-grade glioma. The most notable differences were between PA tumors and pediatric brain tissues. As a cautionary note, for the initial profiling experiments, 3 (of 5) of the nonneoplastic brain samples were obtained from cortex, and most PA arise in the cerebellum or in the optic pathways. We did find the same microRNA expression differences in additional cerebellar samples by qRT-PCR; unfortunately, we were unable to test optic pathway normal samples because of the difficulties in obtaining them as normal controls.

Modest differences between different tumor subsets, by location and histologic and molecular subtypes, were also observed but to a lesser extent. By looking at combined fold change differences and statistical significance, a subset of microRNAs was differentially expressed in NF1-associated PA, compared with tumors with *BRAF* alterations. In addition, the expression differences for miR-21, miR-124, and miR-129 that were subsequently validated by qRT-PCR were more conspicuous in the NF1-PA group. However, because of the relatively small number (4 tumors) tested in this study, the findings must be interpreted with caution and must be validated in the future in larger tumor datasets.

Prior mRNA gene expression studies have identified clear molecular differences in PAs by anatomic site and NF1 status[37,66] and specific transcriptional regulatory networks for PA.[67] Of note, in a recent study, repressed

expression of *ONECUT2* was part of a PA-specific transcriptional network,[67] and we identified it as a predicted target of 2 microRNAs differentially overexpressed in NF1-associated PA.

Our study has revealed some novel, putative oncogene targets that may be specifically upregulated in PA, compared with brain and diffuse gliomas. However, it is possible that specific microRNAs in PA may be regulated by (or regulate) canonical pathways that have been validated to play key roles in PA biology. One such pathway is MAPK, which is constitutively activated in the vast majority of PA by rearrangements and/or mutations involving *BRAF* and its family members.[3,5,6,8,9,12] Of interest, miR-21 is up-regulated by increased MAPK activity in breast cancer[68] and in v-Ki-ras transformed NIH3T3 (DT) cells (compared with nontransformed NIH3T3 cells)[69] and, therefore, acts as a downstream effector in this pathway. As mentioned above, miR-124 is enriched in brain and is evolutionarily conserved even in other species, including snails. In a study focusing on the marine snail *Aplysia*, serotonin downregulated miR-124, an effect that is abolished by MAPK inhibition,[70] suggesting that MAPK is a negative regulator of miR-124. Of interest, through our analysis of functional annotation analysis, we found multiple sets of receptor tyrosine kinase/MAPK/ERK signaling components as possible targets. Collectively, these prior observations and our findings raise the intriguing possibility that MAPK pathway activation leads to alterations in key microRNA levels and that these microRNAs may be important downstream mediators of the pathway in PA and may regulate pathway components. This interesting possibility merits further study.

In summary, we have identified molecular differences based on microRNA expression levels in a large cohort of pediatric PAs, compared with human brain samples. Some investigators have highlighted current limitations in microRNA profiling in pediatric brain tumors,[29] which may require platforms with larger microRNA coverage and increased samples sizes. However, in the current study, we showed the feasibility in profiling as a novel approach to identify relevant targets in PA. Furthermore, we have identified increases in protein levels of putative oncogenes that may be of relevance to PA biology. At the present time, suitable in vivo or in vitro models to follow these observations are lacking but may become available in the near future. Additional studies are needed to confirm our findings and to address the possible functional consequences and clinical relevance for pathologic diagnosis and treatment of patients with PA.

Supplementary Material

Supplementary material is available online at Neuro-Oncology (http://neuro-oncology.oxfordjournals.org/).

Acknowledgments

We thank Wayne Yu for excellent technical assistance.

Funding

This work was supported by the Childhood Brain Tumor Foundation (to F.J.R.), the Pilocytic/Pilomyxoid Astrocytoma Fund (to C.G.E.), the Pediatric Low Grade Astrocytoma Association (to C.G.E.), Ian's Friends Foundation (to M.A.K.), Mayo Clinic CTSA (UL1 RR024150 from the NIH to F.J.R.), and the Mayo Clinic SPORE in Brain Cancer (P50 CA108961 to C.G.). Samples quality assessment and microarray analysis were conducted at The Sidney Kimmel Cancer Center Microarray Core Facility at Johns Hopkins University, supported by National Institutes of Health (P30 CA006973) entitled Regional Oncology Research Center.

Conflict of interest statement. None declared.

References

1. Tihan T, Fisher PG, Kepner JL, et al. Pediatric astrocytomas with monomorphous pilomyxoid features and a less favorable outcome. *J Neuropathol Exp Neurol*. 1999;58(10):1061–1068.
2. Rodriguez FJ, Scheithauer BW, Burger PC, Jenkins S, Giannini C. Anaplasia in pilocytic astrocytoma predicts aggressive behavior. *Am J Surg Pathol*. 2010;34(2):147–160.
3. Bar EE, Lin A, Tihan T, Burger PC, Eberhart CG. Frequent gains at chromosome 7q34 involving BRAF in pilocytic astrocytoma. *J Neuropathol Exp Neurol*. 2008;67(9):878–887.
4. Dougherty MJ, Santi M, Brose MS, et al. Activating mutations in BRAF characterize a spectrum of pediatric low-grade gliomas. *Neuro Oncol*. 2010;12(7):621–630.
5. Jacob K, Albrecht S, Sollier C, et al. Duplication of 7q34 is specific to juvenile pilocytic astrocytomas and a hallmark of cerebellar and optic pathway tumours. *Br J Cancer*. 2009;101(4):722–733.
6. Jones DT, Kocialkowski S, Liu L, et al. Tandem duplication producing a novel oncogenic BRAF fusion gene defines the majority of pilocytic astrocytomas. *Cancer Res*. 2008;68(21):8673–8677.
7. Lin A, Rodriguez FJ, Karajannis MA, et al. BRAF alterations in primary glial and glioneuronal neoplasms of the central nervous system with identification of 2 novel KIAA1549: BRAF fusion variants. *J Neuropathol Exp Neurol*. 2012;71(1):66–72.
8. Pfister S, Janzarik WG, Remke M, et al. BRAF gene duplication constitutes a mechanism of MAPK pathway activation in low-grade astrocytomas. *J Clin Invest*. 2008;118(5):1739–1749.
9. Sievert AJ, Jackson EM, Gai X, et al. Duplication of 7q34 in pediatric low-grade astrocytomas detected by high-density single-nucleotide polymorphism-based genotype arrays results in a novel BRAF fusion gene. *Brain Pathol*. 2009;19(3):449–458.

10. Yu J, Deshmukh H, Gutmann RJ, et al. Alterations of BRAF and HIPK2 loci predominate in sporadic pilocytic astrocytoma. *Neurology*. 2009;73(19):1526–1531.
11. Cin H, Meyer C, Herr R, et al. Oncogenic FAM131B-BRAF fusion resulting from 7q34 deletion comprises an alternative mechanism of MAPK pathway activation in pilocytic astrocytoma. *Acta Neuropathol*. 2011;121(6):763–774.
12. Jones DT, Kocialkowski S, Liu L, Pearson DM, Ichimura K, Collins VP. Oncogenic RAF1 rearrangement and a novel BRAF mutation as alternatives to KIAA1549:BRAF fusion in activating the MAPK pathway in pilocytic astrocytoma. *Oncogene*. 2009;28(20):2119–2123.
13. Rodriguez FJ, Perry A, Gutmann DH, et al. Gliomas in neurofibromatosis type 1: a clinicopathologic study of 100 patients. *J Neuropathol Exp Neurol*. 2008;67(3):240–249.
14. Jones DT, Gronych J, Lichter P, Witt O, Pfister SM. MAPK pathway activation in pilocytic astrocytoma. *Cell Mol Life Sci*. 2012;69(11): 1799–1811.
15. Chan JA, Krichevsky AM, Kosik KS. MicroRNA-21 is an antiapoptotic factor in human glioblastoma cells. *Cancer Res*. 2005;65(14):6029–6033.
16. Ciafre SA, Galardi S, Mangiola A, et al. Extensive modulation of a set of microRNAs in primary glioblastoma. *Biochem Biophys Res Commun*. 2005;334(4):1351–1358.
17. Kefas B, Godlewski J, Comeau L, et al. microRNA-7 inhibits the epidermal growth factor receptor and the Akt pathway and is down-regulated in glioblastoma. *Cancer Res*. 2008;68(10):3566–3572.
18. Medina R, Zaidi SK, Liu CG, et al. MicroRNAs 221 and 222 bypass quiescence and compromise cell survival. *Cancer Res*. 2008;68(8):2773–2780.
19. Shi L, Cheng Z, Zhang J, et al. hsa-mir-181a and hsa-mir-181b function as tumor suppressors in human glioma cells. *Brain Res*. 2008;1236:185–193.
20. Sumazin P, Yang X, Chiu HS, et al. An extensive microRNA-mediated network of RNA-RNA interactions regulates established oncogenic pathways in glioblastoma. *Cell*. 2011;147(2):370–381.
21. Li D, Chen P, Li XY, et al. Grade-specific expression profiles of miRNAs/mRNAs and docking study in human grade I-III astrocytomas. *Omics*. 2011;15(10):673–682.
22. Nicoloso MS, Calin GA. MicroRNA involvement in brain tumors: from bench to bedside. *Brain pathology (Zurich, Switzerland)*. 2008;18(1):122–129.
23. Lu J, Getz G, Miska EA, et al. MicroRNA expression profiles classify human cancers. *Nature*. 2005;435(7043):834–838.
24. White FV, Anthony DC, Yunis EJ, Tarbell NJ, Scott RM, Schofield DE. Nonrandom chromosomal gains in pilocytic astrocytomas of childhood. *Hum Pathol*. 1995;26(9):979–986.
25. Cioffi JA, Yue WY, Mendolia-Loffredo S, Hansen KR, Wackym PA, Hansen MR. MicroRNA-21 overexpression contributes to vestibular schwannoma cell proliferation and survival. *Otol Neurotol*. 2010;31(9):1455–1462.
26. Erkan EP, Breakefield XO, Saydam O. miRNA signature of schwannomas: possible role(s) of 'tumor suppressor' miRNAs in benign tumors. *Oncotarget*. 2011;2(3):265–270.
27. Saydam O, Senol O, Wurdinger T, et al. miRNA-7 attenuation in Schwannoma tumors stimulates growth by upregulating three oncogenic signaling pathways. *Cancer Res*. 2011;71(3):852–861.
28. Birks DK, Barton VN, Donson AM, Handler MH, Vibhakar R, Foreman NK. Survey of MicroRNA expression in pediatric brain tumors. *Pediatr Blood Cancer*. 2011;56(2):211–216.
29. Sredni ST, Huang CC, Bonaldo Mde F, Tomita T. MicroRNA expression profiling for molecular classification of pediatric brain tumors. *Pediatr Blood Cancer*. 2011;57(1):183–184.
30. Costa FF, Bischof JM, Vanin EF, et al. Identification of microRNAs as potential prognostic markers in ependymoma. *PLoS One*. 2011;6(10):e25114.
31. Cahill S, Smyth P, Denning K, et al. Effect of BRAFV600E mutation on transcription and post-transcriptional regulation in a papillary thyroid carcinoma model. *Mol Cancer*. 2007;6:21.
32. Croce CM, Calin GA. miRNAs, cancer, and stem cell division. *Cell*. 2005;122(1):6–7.
33. Wang H, Ach RA, Curry B. Direct and sensitive miRNA profiling from low-input total RNA. *RNA*. 2007;13(1):151–159.
34. Winer J, Jung CK, Shackel I, Williams PM. Development and validation of real-time quantitative reverse transcriptase-polymerase chain reaction for monitoring gene expression in cardiac myocytes in vitro. *Anal Biochem*. 1999;270(1):41–49.
35. Lewis BP, Burge CB, Bartel DP. Conserved seed pairing, often flanked by adenosines, indicates that thousands of human genes are microRNA targets. *Cell*. 2005;120(1):15–20.
36. Ross AE, Marchionni L, Vuica-Ross M, et al. Gene expression pathways of high grade localized prostate cancer. *Prostate*. 2011;71(14):1568–1577.
37. Rodriguez FJ, Giannini C, Asmann YW, et al. Gene expression profiling of NF-1-associated and sporadic pilocytic astrocytoma identifies aldehyde dehydrogenase 1 family member L1 (ALDH1L1) as an underexpressed candidate biomarker in aggressive subtypes. *J Neuropathol Exp Neurol*. 2008;67(12):1194–1204.
38. McCall MN, Bolstad BM, Irizarry RA. Frozen robust multiarray analysis (fRMA). *Biostatistics*. 2010;11(2):242–253.
39. Papagiannakopoulos T, Shapiro A, Kosik KS. MicroRNA-21 targets a network of key tumor-suppressive pathways in glioblastoma cells. *Cancer Res*. 2008;68(19):8164–8172.
40. Chan JA, Krichevsky AM, Kosik KS. MicroRNA-21 is an antiapoptotic factor in human glioblastoma cells. *Cancer Res*. 2005;65(14):6029–6033.
41. Chen Y, Liu W, Chao T, et al. MicroRNA-21 down-regulates the expression of tumor suppressor PDCD4 in human glioblastoma cell T98G. *Cancer Lett*. 2008;272(2):197–205.
42. Li Y, Li W, Yang Y, et al. MicroRNA-21 targets LRRFIP1 and contributes to VM-26 resistance in glioblastoma multiforme. *Brain Res*. 2009;1286:13–18.
43. Gabriely G, Wurdinger T, Kesari S, et al. MicroRNA 21 promotes glioma invasion by targeting matrix metalloproteinase regulators. *Mol Cell Biol*. 2008;28(17):5369–5380.
44. Baraniskin A, Kuhnhenn J, Schlegel U, et al. Identification of microRNAs in the cerebrospinal fluid as biomarker for the diagnosis of glioma. *Neuro Oncol*. 2012;14(1):29–33.
45. Rodriguez EF, Scheithauer BW, Giannini C, et al. PI3K/AKT pathway alterations are associated with clinically aggressive and histologically anaplastic subsets of pilocytic astrocytoma. *Acta Neuropathol*. 2011;121(3):407–420.
46. Silber J, Lim DA, Petritsch C, et al. miR-124 and miR-137 inhibit proliferation of glioblastoma multiforme cells and induce differentiation of brain tumor stem cells. *BMC Med*. 2008;6:14.
47. Rhee JW, Arata A, Selleri L, et al. Pbx3 deficiency results in central hypoventilation. *Am J Pathol*. 2004;165(4):1343–1350.
48. Rottkamp CA, Lobur KJ, Wladyka CL, Lucky AK, O'Gorman S. Pbx3 is required for normal locomotion and dorsal horn development. *Dev Biol*. 2008;314(1):23–39.

49. Takahashi K, Liu FC, Oishi T, et al. Expression of FOXP2 in the developing monkey forebrain: comparison with the expression of the genes FOXP1, PBX3, and MEIS2. *J Comp Neurol*. 2008;509(2):180–189.
50. Kaoru T, Liu FC, Ishida M, et al. Molecular characterization of the intercalated cell masses of the amygdala: implications for the relationship with the striatum. *Neuroscience*. 2010;166(1):220–230.
51. Li Z, Huang H, Li Y, et al. Up-regulation of a HOXA-PBX3 homeobox-gene signature following down-regulation of miR-181 is associated with adverse prognosis in patients with cytogenetically-abnormal AML. *Blood*. 2012;119(10):2314–2324.
52. Ramberg H, Alshbib A, Berge V, Svindland A, Tasken KA. Regulation of PBX3 expression by androgen and Let-7d in prostate cancer. *Mol Cancer*. 2011;10:50.
53. Datta B, Majumdar A, Datta R, Balusu R. Treatment of cells with the angiogenic inhibitor fumagillin results in increased stability of eukaryotic initiation factor 2-associated glycoprotein, p67, and reduced phosphorylation of extracellular signal-regulated kinases. *Biochemistry*. 2004;43(46):14821–14831.
54. Dasgupta B, Yi Y, Hegedus B, Weber JD, Gutmann DH. Cerebrospinal fluid proteomic analysis reveals dysregulation of methionine aminopeptidase-2 expression in human and mouse neurofibromatosis 1-associated glioma. *Cancer Res*. 2005;65(21):9843–9850.
55. Sin N, Meng L, Wang MQ, Wen JJ, Bornmann WG, Crews CM. The anti-angiogenic agent fumagillin covalently binds and inhibits the methionine aminopeptidase, MetAP-2. *Proc Natl Acad Sci USA*. 1997;94(12):6099–6103.
56. Sawanyawisuth K, Wongkham C, Pairojkul C, et al. Methionine aminopeptidase 2 over-expressed in cholangiocarcinoma: potential for drug target. *Acta Oncol*. 2007;46(3):378–385.
57. Selvakumar P, Lakshmikuttyamma A, Dimmock JR, Sharma RK. Methionine aminopeptidase 2 and cancer. *Biochim Biophys Acta*. 2006;1765(2):148–154.
58. Catalano A, Romano M, Robuffo I, Strizzi L, Procopio A. Methionine aminopeptidase-2 regulates human mesothelioma cell survival: role of Bcl-2 expression and telomerase activity. *Am J Pathol*. 2001;159(2):721–731.
59. Sheen IS, Jeng KS, Jeng WJ, et al. Fumagillin treatment of hepatocellular carcinoma in rats: an in vivo study of antiangiogenesis. *World J Gastroenterol*. 2005;11(6):771–777.
60. Hannig G, Lazarus DD, Bernier SG, et al. Inhibition of melanoma tumor growth by a pharmacological inhibitor of MetAP-2, PPI-2458. *Int J Oncol*. 2006;28(4):955–963.
61. Dooley AL, Winslow MM, Chiang DY, et al. Nuclear factor I/B is an oncogene in small cell lung cancer. *Genes Dev*. 2011;25(14):1470–1475.
62. Moon HG, Hwang KT, Kim JA, et al. NFIB is a potential target for estrogen receptor-negative breast cancers. *Mol Oncol*. 2011;5(6):538–544.
63. Mitani Y, Rao PH, Futreal PA, et al. Novel chromosomal rearrangements and break points at the t(6;9) in salivary adenoid cystic carcinoma: association with MYB-NFIB chimeric fusion, MYB expression, and clinical outcome. *Clin Cancer Res*. 2011;17(22):7003–7014.
64. Wetterskog D, Lopez-Garcia MA, Lambros MB, et al. Adenoid cystic carcinomas constitute a genomically distinct subgroup of triple-negative and basal-like breast cancers. *J Pathol*. 2012;226(1):84–96.
65. Baek D, Villen J, Shin C, Camargo FD, Gygi SP, Bartel DP. The impact of microRNAs on protein output. *Nature*. 2008;455(7209):64–71.
66. Sharma MK, Mansur DB, Reifenberger G, et al. Distinct genetic signatures among pilocytic astrocytomas relate to their brain region origin. *Cancer Res*. 2007;67(3):890–900.
67. Deshmukh H, Yu J, Shaik J, et al. Identification of transcriptional regulatory networks specific to pilocytic astrocytoma. *BMC Med Genomics*. 2011;4:57.
68. Huang TH, Wu F, Loeb GB, et al. Up-regulation of miR-21 by HER2/neu signaling promotes cell invasion. *J Biol Chem*. 2009;284(27):18515–18524.
69. Loayza-Puch F, Yoshida Y, Matsuzaki T, Takahashi C, Kitayama H, Noda M. Hypoxia and RAS-signaling pathways converge on, and cooperatively downregulate, the RECK tumor-suppressor protein through microRNAs. *Oncogene*. 2010;29(18):2638–2648.
70. Rajasethupathy P, Fiumara F, Sheridan R, et al. Characterization of small RNAs in Aplysia reveals a role for miR-124 in constraining synaptic plasticity through CREB. *Neuron*. 2009;63(6):803–817.